

# Walk-to-brachiate Transfer of Multi-Locomotion Robot with Error Recovery

Zhiguo Lu, Tadayoshi Aoyama, Kosuke Sekiyama, Yasuhisa Hasegawa, and Toshio Fukuda

**Abstract**—This paper describes walk-to-brachiate transfer of a multi-locomotion robot (MLR). The MLR has multiple types of locomotion such as biped walking, quadruped walking and brachiation. This transfer is carried out through vertical ladder climbing as the robot must raise its body to start brachiating. As a result we have designed two stable transfer motions from walk to climb and from climb to brachiate, while contact situations and constraints of the robot are changing during the transfers. In addition, we have proposed a control algorithm by considering the reaction force from environment, and the setting of parameter is based on a kinetic model of the robot in order to tolerate relative position errors between the robot and its environments such as rungs of the ladder. The robustness of the designed motions with error corrections is experimentally verified.

## I. INTRODUCTION

In recent years, a lot of moving motions have been researched to make a robot move naturally like an animal, such as biped walking [1], quadruped walking [2], brachiation [3]. However, these motions are performed by different robots and most of the robots have a single type of locomotion. As is known to all, the environment in the world is dynamic. It is not enough to adapt to different situations for only one type of moving motion. There are some researchers who have dealt with this problem. Kanehiro et al. [4] have proposed a method to alter the locomotion style to pass through narrow spaces. In our laboratory, Fukuda et al. [5] have developed an anthropoid-like “Multi-Locomotion Robot (MLR)” shown in Fig. 1. MLR is a novel, bio-inspired robot that can perform in stand-alone several kinds of locomotion. In past years, we have realized some types of locomotion separately, such as biped walking on flat terrain [6], quadruped walking on a slope [7], brachiation on horizontal ladder [8] and vertical ladder climbing [9].

In this paper, we focus on the transfer from walk to brachiation to connect the previous independent motions. The walk-to-brachiate transfer needs complex motions with arms and legs. The arm/leg cooperation has been explained in humanoid robots whose hands touch an environment [10]. Harada et al. generated whole body motion for a pushing task through cooperating arm and leg moments [11]. There are some works generating of the body motion in order to increase arm manipulability and robot stability [12].

Z. LU, T. AOYAMA, K. SEKIYAMA, T. FUKUDA are with the Department of Micro-Nano Systems Engineering, Nagoya University, Furo-cho-1, Chikusa-ku, Nagoya, 464-8603, Japan. luzhiguo, aoyama@robo.mein.nagoya-u.ac.jp, sekuyama, fukuda@mein.nagoya-u.ac.jp

Y. HASEGAWA is with Mechanical system engineering, University of Tsukuba, 1-1-1 Tenodai, Tsukuba, 305-8573, Japan. hase@esys.tsukuba.ac.jp

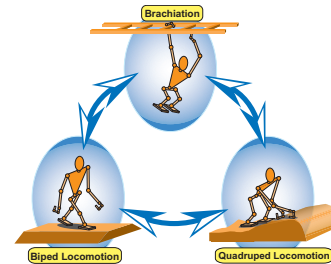


Fig. 1. Concept of multi-locomotion robot.

In addition, the HRP-2 robot has realized walking on a rough terrain by use of a handrail [13]. However, these conventional body motions are based on the condition that the robots move on the ground. The situation that we consider is not only on the ground, but also a vertical and horizontal ladder. In this situation, a robot falling down from the ladder may happen even if a small error exists. Thus, we propose a control algorithm by considering the reaction force from its environment, and the setting of parameter is based on a kinetic model of the robot in order to tolerate relative position errors between the robot and its environments such as rungs of the ladder. Finally, we realize the transfer motions from walk to climb and from climb to brachiate by applying the proposed control algorithm, and the robustness of the designed motions with error corrections are experimentally verified.

## II. MOTION DESIGN

The motion design is based on a prototype of the MLR-Gorilla robot III [5]. Its height is approx 1.0 m, and weight is approx 24 kg. There are 24 degrees of freedom on the whole body. The link structure is shown in Fig. 2.

### A. Connected Posture

The transition motion flow from biped walking to brachiation is shown in Fig. 3. Biped standing (Fig. 3. a) is taken

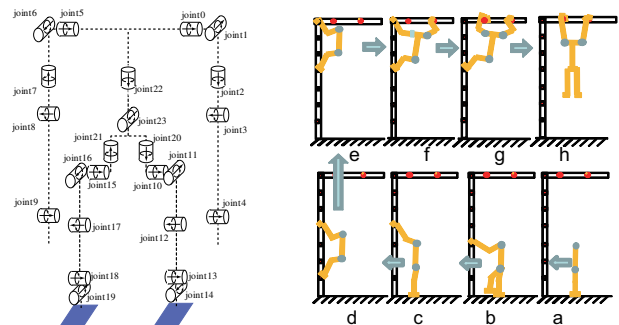


Fig. 2. Link structure of Gorilla III Fig. 3. Transition motion flow

as the end posture of biped walking and the robot getting on the ladder with two hands and two legs (Fig. 3. d) is looked as the start posture of ladder climbing. The end posture of ladder climbing is two feet stepping on one rung and two hands grasping on the upper rung (Fig. 3. e). The initial posture of brachiation is hanging on the horizontal ladder with two hands (Fig. 3. h).

### B. Motion Flow

The MLR stands in front of the ladder at biped posture and the related information about the ladder is given beforehand. The distance from the MLR to the ladder is within arms reach. In this condition, the transition motion can be divided into seven steps. The motion flow from biped standing to brachiation is as follows:

- 1) Raise hands to grasp the rung of the vertical ladder.
- 2) Walk close to the ladder with hands gripping the rung (Fig. 3. b-c).
- 3) Step on the ladder (Fig. 3.d).
- 4) Climb up on the vertical ladder [9] (Fig. 3. d-e).
- 5) Turn shoulder to grasp the horizontal rung (Fig. 3. e-f).
- 6) Move the other hand to horizontal rung (Fig. 3. f-g).
- 7) Move legs away from the ladder and extend arms straight (Fig. 3. g-h).

### III. CONTROL ALGORITHM

In the transition motions, there are always some errors from the initial posture, precision of environmental parameters and external disturbances. These errors are unavoidable.

In position control, the position errors directly influence the contact situation. There are two evaluation factors for the contact situation. One is the position error between the end effector and the target supporting point. Another is the reaction force from the supporting point.

There are two methods to adjust the contact situation: one is the position adjustment method; another is the force adjustment method. These error recovery methods are proposed for motion control.

#### A. Control Algorithm with Position Adjustment Method in the Motion of Walking Close to the Ladder

We use position adjustment measure to adjust the contact situation of hands when the robot walks close to the ladder. The unstable problems such as falling down towards one side and rotation around the axis of yaw (AOY) can be prevented. AOY is denoted in Fig. 4. The gripping situation of hands is judged by the feedback of force sensors. The force sensors are installed on the forearms. The force on vertical direction shown in Fig. 5 is calculated in (1). First, the robot raises its hands over the ladder's rung. Next, the robot descends its hands to get in touch with the rung of the ladder. The threshold level of force gradient is expressed in (2). The robot starts to grip the rung of the ladder when the force gradient is more than  $\varepsilon_d = 0.5$  N, where  $\varepsilon_d$  is chosen heuristically. After that the robot does the next motion.

$$F_t = F_z \cos \theta - F_y \sin \theta, \quad (1)$$

$$\varepsilon = F_t - F_{t-\Delta t}. \quad (2)$$

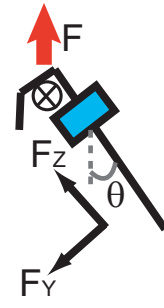
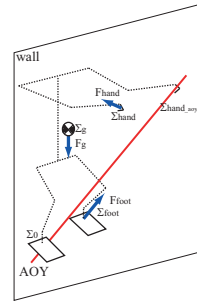


Fig. 4. Model of body balance

Fig. 5. Force sensor on arm.

The reaction forces of hands can be changed by moving the body. For example, if the robot has a tendency to turn right, the reaction force of the left hand will be smaller than right hand. Next the robot body moves left to reduce this tendency. In contrast the robot body should move right. In addition, if both hands' forces are below 0 N, the robot body adjusts by moving down. So the gripping situation can be adjusted by changing the position of COG relative to the support points (Video is shown in Fig. 20).

The control flow is shown in Fig. 6:

- 1) Both hands grip the ladder.
- 2) Judge the value from two force sensors on forearms.
- 3) Adjust the body position based to the touch situation.
- 4) If the forces of both hands are over 0, then continue to do the motion, else go back to 2).

#### B. Kinematic Calculation for Turning Around motion

In the transition motion from ladder climbing to brachiation we don't want to change the trajectory of the robot's COG. So we use a force adjustment measure to adjust ladder and right hand grasping the upper rung in the whole turning motion. Since the robot keeps two feet stepping on one rung and the right hand grasping on the upper rung, we need to make the distance from hand to feet not to change. The turning shoulder motion for the upper body was designed in the lateral plane. The symmetrical motion is designed as follows:

- 1) Move right hand to grasp the rung's center with two legs stepping on the vertical ladder.
- 2) Turn shoulder left.
- 3) Grasp the second horizontal rung.

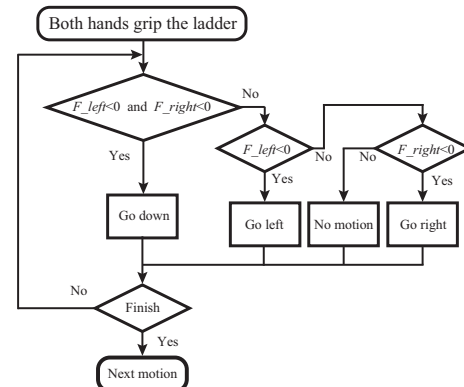


Fig. 6. The control algorithm of body adjustment.

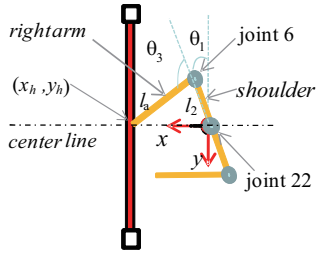


Fig. 7. Turning shoulder motion.

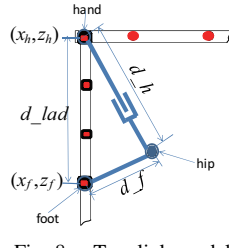


Fig. 8. Two-link model.

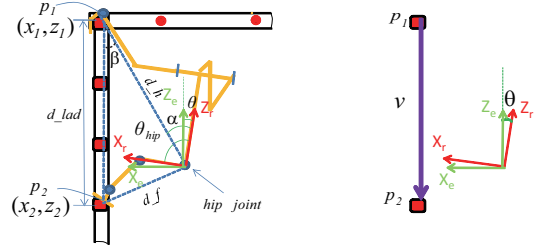


Fig. 9. Coordinate systems of robot and environment

In the motion of turning shoulder left, we only change two joints angle:  $\theta_1$  and  $\theta_3$  (Fig. 7). Where  $\theta_1$  is the angle of waist joint(joint 22) and  $\theta_3$  is the roll joint on shoulder(joint 6) (Fig. 2). Note that, the pitch joint on shoulder (joint 5) is 90 degree in the turning shoulder motion. We design the motion of the upper body like this: the right hand grasping the rung's center and waist moving along the ladder's center line. The yaw angle of shoulder  $\theta_3$  can be expressed as a function of turning shoulder angle  $\theta_1$ ,

$$\theta_3 = \frac{\pi}{2} + \arcsin\left(\frac{l_2 \cos \theta_1}{l_a}\right) - \theta_1 := F_{\theta_3}(\theta_1), \quad (3)$$

where  $l_2$  is half width of the shoulder.  $l_a$  is the horizontal distance from the right shoulder to right hand. The distance from the right hand to foot should be same as the distance of bars that are separately contacted with the robot's hand and feet. The fixed distance is maintained by adjusting the angle of hip motor-the other motors' angle on the legs is fixed. In this case the distance from foot to hip ( $d_{-f}$ ) is constant. However, the distance from grasping hand to the hip ( $d_{-h}$ ) is changed. Therefore the turning shoulder left motion can be simplified as the two-link model (Fig. 8). In the two-link model, we need to calculate the desired angle of hip joint.

The position of foot relative to original point of robot coordinate system is necessary for hip angle calculation. The robot coordinate system changes in the transition motion. The vector from  $p_1$  to  $p_2$  (Fig. 9) relative to environment coordinate system (coordinate system e) is expressed as:

$${}^e \mathbf{v} = {}^e \mathbf{p}_2 - {}^e \mathbf{p}_1 = \begin{bmatrix} x_{12} \\ 0 \\ z_{12} \end{bmatrix} \quad (4)$$

where,  $x_{12}$  and  $z_{12}$  are the position parameters which are given beforehand or recognized by the robot. Robot coordinate system (r) can be taken through rotating the environment coordinate system (e) about  $Y_e$  by  $-\theta$ .

$$\theta = \alpha - \beta, \quad (5)$$

where,

$$\alpha = \arctan\left(\frac{x_1}{z_1}\right), \quad (6)$$

$$\beta = \arccos\left(\frac{d_{-bar}^2 + d_{-h}^2 - d_{-f}^2}{2d_{-bar}d_{-h}}\right), \quad (7)$$

$$d_{-h} = \sqrt{x_1^2 + z_1^2}, \quad (8)$$

$$d_{-bar} = \sqrt{x_{12}^2 + z_{12}^2}, \quad (9)$$

where  $p_1$  and  $p_2$  denote the positions of right hand and the center position of two feet.  $d_f$  is the length of second link which is a constant value. The vector relative to coordinate r:  ${}^r \mathbf{v}$  can be obtained by rotating  ${}^e \mathbf{v}$  about  $Y_r$  by  $\theta$ :

$${}^r \mathbf{v} = {}^e \mathbf{R} {}^e \mathbf{v} = \begin{bmatrix} \cos \theta & 0 & \sin \theta \\ 0 & 1 & 0 \\ -\sin \theta & 0 & \cos \theta \end{bmatrix} \begin{bmatrix} x_{12} \\ 0 \\ z_{12} \end{bmatrix} \quad (10)$$

The position of the stepped rung relative to coordinate system r is expressed as:

$${}^r \mathbf{p}_2 = {}^r \mathbf{p}_1 + {}^r \mathbf{v} = \begin{bmatrix} x_2 \\ 0 \\ z_2 \end{bmatrix}, \quad (11)$$

where,  ${}^r \mathbf{p}_1 = [x_1, 0, z_1]^T$  is the position of the right hand relative to the coordinate system r, which is calculated by using kinematics according to the feedback angles of the robot joints, and then, the following equation is obtained by substituting  ${}^r \mathbf{p}_1$  into (11),

$$x_2 = x_1 + x_{12} \cos \theta + z_{12} \sin \theta, \quad (12)$$

$$z_2 = z_1 - x_{12} \sin \theta + z_{12} \cos \theta, \quad (13)$$

where,  $x_{12}$  and  $z_{12}$  are parameters of the ladder, which are given beforehand.  $z_1$  is the position element of right hand which can be expressed by  $\theta_1$ . In the turning left motion, we only adjust one angle of hips on legs:  $\theta_{hip}$ . The other joints on legs keep on fixed angles and the value of each angle can be read from the encoder. By substituting the fixed angles and  $z_2$  into kinematic equations we can obtain angle of hip joint:

$$\theta_{hip} = 2 \arctan\left(\frac{A - \sqrt{B^2 + 4C^2 - 4z_2^2}}{2(D - z_2)}\right) := F_{unc\theta_{hip}}(\theta_1), \quad (14)$$

note that  $A, B, C$  and  $D$  are constant and  $z_2$  is the function of  $\theta_1$ . Where,

$$A = -2l_{d5}S_{18} - 2C_{18}C_{19}l_{d5}S_{17} - 2C_{17}C_{18}l_{d5}S_{18}, \quad (15)$$

$$B = 2l_{d4}S_{17} + 2C_{18}C_{19}l_{d5}S_{18}, \quad (16)$$

$$C = (C_{16}C_{17}l_{d4} + C_{16}C_{17}C_{18}C_{19}l_{d5} - l_{d3}S_{16} - C_{16}C_{19}l_{d5}S_{17}S_{18} + l_{d5}S_{18}S_{19})^2, \quad (17)$$

$$D = C_{16}C_{17}l_{d4} + C_{16}C_{17}C_{18}C_{19}l_{d5} - l_{d5}S_{18} + l_{d5}S_{16}S_{19}, \quad (18)$$

where  $S_i = \sin(\theta_i)$ ,  $C_i = \cos(\theta_i)$ .  $\theta_i$  are angles of fixed joint  $i$  on leg.  $l_{di}$  is the length parameter of links on leg. Until now,

we got the functions of  $\theta_3$ , and  $\theta_{hip}$  about  $\theta_1$ . Other angles are certain values. So, we can obtain the position function  $P(\theta_1)$ :

$$P(\theta_1) = (\theta_i(\theta_1), \mathbf{p}_{ef}(\theta_1), \mathbf{p}_i(\theta_1), \mathbf{r}_i(\theta_1), \hat{\mathbf{z}}_i(\theta_1)), \quad (19)$$

where  $i$  is the joint number:  $i=1,2, \dots, 24$ .  $ef$  is the number of end effector which can be right hand ( $rh$ ), left hand ( $lh$ ), right foot ( $rf$ ) and left foot ( $lf$ ).  $\theta_i(\theta_1)$  is the angle of the  $i$ th joint.  $\mathbf{p}_{ef}(\theta_1)$  and  $\mathbf{p}_i(\theta_1)$  are respectively  $3 \times 1$  position vectors of  $ef$ th effectors and  $i$ th joint.  $\mathbf{r}_i(\theta_1)$  is a  $3 \times 1$  position vector from the  $i$ th joint to its nearest end effector  $ef$ th end effector.  $\hat{\mathbf{z}}_i(\theta_1)$  is a  $3 \times 1$  unit direction vector of  $i$ th joint relative to environment coordinate system.

### C. Control Algorithm with Force Adjustment Method

The turning shoulder left motion can be realized by applying a pure position control to the position element  $\theta_i(\theta_{1t})$ . However the unavoidable position errors will lead the success rate very low. Even with a small position error, a large change of supporting force on end effectors will be produced. Sometimes most of the weight load on arm and the gripping motor will be overloaded (Fig. 10). Some other times the legs supporting too much of the weight and the non-symmetrical errors will lead one of the hip motors being overloaded (Fig. 11).

In order to solve the above problems, the contact situation adjustment measure is used to change the supporting forces of the end effectors. The control flow is shown in Fig. 12.

The robot motion is designed by using position control with inverse kinematic method. And then we change two hip joints (on pitch direction) from position control to force control. We call the hip joints as key joints. The key joints

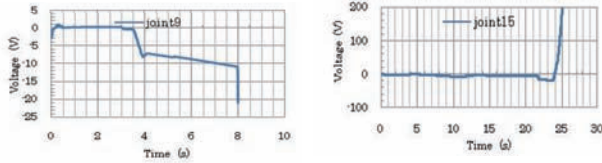


Fig. 10. Gripping motor overload. Fig. 11. Right hip motor overload.

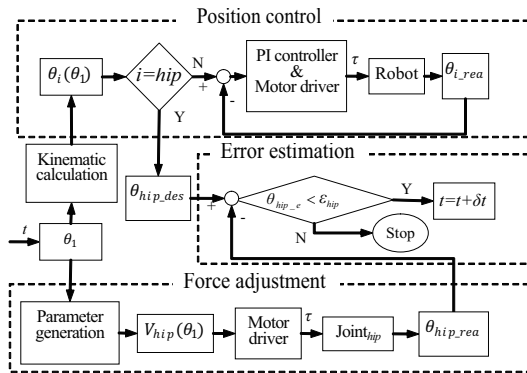


Fig. 12. The control chart with force adjustment.  $t$  is the time parameter.  $\theta_i(\theta_1)$  are the angle functions of joint  $i$  about angles and real angles of joint  $i$ .  $e$  and  $\tau$  are the angle error and torque of joint.  $\epsilon_{hip}$  is experimentally decided parameter denoting the limited angle error of hip joint.

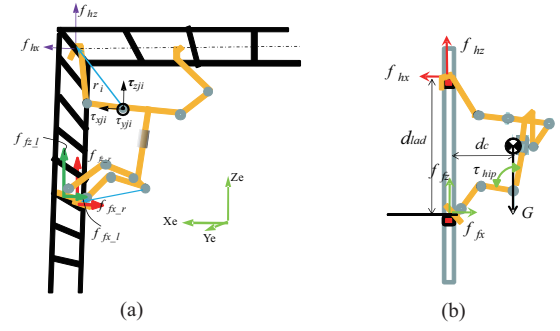


Fig. 13. Forces in turning shoulder motion (a)3-D model (b) sagittal view.

focus on how to allocate the weight to arm and legs, and how to prevent the other motors being overloaded. The shoulder angle  $\theta_1$  changes according to the time parameter.  $\theta_i(\theta_1)$  is the designed angle of each joint. The contact situation is adjusted by setting the optimal voltage  $v_{hip}$  to the hip motors. The position errors are evaluated by the angle error of hip joint  $\theta_{hip-e}$ .

### D. Parameter Setting for Force Adjustment Method

The most important thing is how to adjust the torque of the other motors by changing the voltage of hip motors. And how much voltage is suitable. In order to solve these problems we need to analyze the force first.

The robot is supported by two feet and right hand on the ladder. We abstract the force model as Fig. 13. The whole gravity  $G$  loads on the COG. The inertia force is small enough relative to  $G$ , so we ignore it. The robot steps on the rung symmetrically. So we make an assumption that the reaction forces of right foot equal to left foot:  $\mathbf{f}_{rf} = \mathbf{f}_{lf}$  and then we set  $\mathbf{f}_{fx} = 2\mathbf{f}_{rf} = 2\mathbf{f}_{lf}$ . We design the supporting force on Y direction as 0 to prevent the foot sliding aside on the rung. Analyze the forces of the whole body. We can obtain the following equations:

$$f_{fx} + f_{hx} = 0, \quad (20)$$

$$f_{fz} + f_{hz} - G = 0, \quad (21)$$

$$f_{fz}d_{lad} - Gd_c = 0. \quad (22)$$

From (20), (21), and (22) we can obtain:

$$\mathbf{f}_{rh} = [f_{hx}, f_{hy}, f_{hz}]^T = \begin{bmatrix} Gd_c/d_{lad}, 0, G - f_{fz} \end{bmatrix}^T, \quad (23)$$

$$\mathbf{f}_{rf} = \mathbf{f}_{lf} = \frac{[f_{fx}, f_{fy}, f_{fz}]^T}{2} = \begin{bmatrix} -Gd_c/2d_{lad}, 0, f_{fz}/2 \end{bmatrix}^T. \quad (24)$$

From (23), (24), we can find that the supporting forces on X direction are decided by  $G$  and  $d_{lad}$ . And the forces are certain when the robot moves as a certain trajectory; however, the forces on Z direction can be adjusted by changing the value of  $f_{fz}$ . We will explain how to change  $f_{fz}$  and how to adjust the motors' torques in the sub section.

The torques of each joint can be calculated as the follows:

$$\tau_i = \mathbf{r}_i \times \mathbf{f}_{sup_n} \cdot \hat{\mathbf{z}}_i, \quad (25)$$

where  $\mathbf{f}_{sup_n}$  is the supporting force of the end effector near to the  $i$ th joint  $sup_n = rf, lf, rh$  or  $lh$ .  $\mathbf{r}_i$  and  $\hat{\mathbf{z}}_i$  are position

factors which are mentioned in (19). When  $i = rhip$ (joint of right hip) (25) can be written as:

$$\tau_{rhip} = \mathbf{r}_{rhip} \times \mathbf{f}_{rf} \cdot \hat{\mathbf{z}}_{rhip}, \quad (26)$$

By solving (26) we can express foot supporting force by  $\tau_{rhip}$ .

$$\mathbf{f}_{rfz} = \frac{Gd_c r_{rfz} + 2\tau_{rhip} d_{lad}}{2r_{rfx} d_{lad}}. \quad (27)$$

We set the left foot supply the same force and set the same hip torques as  $\tau_{hip}$ . Then, we can obtain the following equation:

$$f_{fz} = f_{rfz} + f_{lfz} = 2f_{rfz} = \frac{Gd_c r_{rfz} + 2\tau_{hip} d_{lad}}{r_{rfx} d_{lad}}, \quad (28)$$

By observing (28), we can find  $f_{fz}$  can be adjusted by changing the torque of hip joint  $\tau_{hip}$ . The other parameters in (28) are certain and can be obtained from (19). Because  $\theta_1$  is the only variable of (19) the motors torques  $\tau_i$  can be expressed as a two variable function

$$\tau_i := F_{\tau_i}(\theta_1, \tau_{hip}). \quad (29)$$

In our experimental environment, an experimental joint torque  $\tau_i$  is proportional to the voltage of motor  $v_i$  for the motor driver; also, the proportionality constant is  $\frac{\tau_{ri}}{3}$ , where  $\tau_{ri}$  is the rated torque of motor  $i$ . Then, the relationship between  $v_i$  and  $\tau_i$  is given as follows:

$$v_i := \frac{3\tau_i}{\tau_{ri} m_i}, \quad (30)$$

where  $m_i$  is the gear ratio. The safe range of motor voltage  $v_i$  is from -10 V to 10 V. If the absolute value of  $v_i$  is more than 10, the motor will be overloaded. The related function between  $v_i$  and  $v_{hip}$  is obtained by substituting (30) into (29)

$$v_i := F_{v_i}(\theta_1, \tau_{hip}). \quad (31)$$

The voltage of motors will change according to the voltage of hip motors  $v_{hip}$  even if the robot posture doesn't change. Here we take the posture  $\theta_1 = 0$  as an example. Fig. 14 shows the voltages of motors when  $v_{hip}$  changes from 0 V to 10 V. From Fig. 14, we can find the absolute voltages change as the changing of  $v_{hip}$ . The motor with the maximum voltage is in most danger of being overloaded and is called the critical motor. The voltage of the critical motor  $v_{crit}$  is

$$v_{crit} = \max(v_i) := F_{maxv_i}(\theta_1, v_{hip}). \quad (32)$$

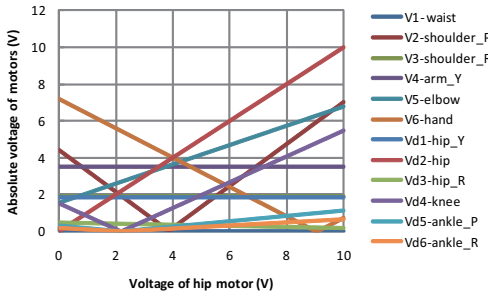


Fig. 14. Voltages of motors adjusted by hip voltage.

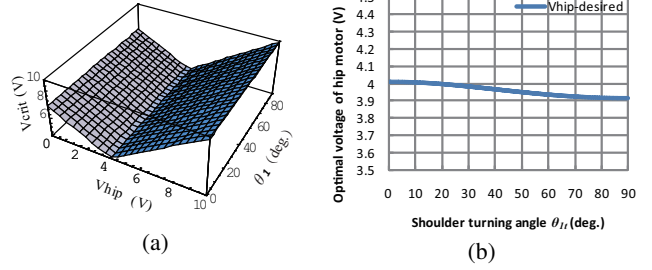


Fig. 15. Optimal voltage of hip motor in turning shoulder motion. (a) 3-D surface graphics of critical motor's voltage. (b) optimal voltage in turning shoulder left motion.

The principle is minimizing the voltage of critical motor because we want to prevent the motors being overloaded. The critical motor gets the minimum voltage when  $v_{hip} = 4.012$ . So the 4.012 V is the optimal voltage in the posture  $\theta_1 = 0$ . In the same principle we can calculate the other optimal voltages of hip motor. From (32) we can obtain the relationship of  $v_{crit}, \theta_1$  and  $v_{hip}$ . The surface graphics is shown in Fig. 15 (a). The hip voltage can get an optimal value when  $v_{crit}$  gets the minimum value. The optimal voltage of hip motor about shoulder angle  $\theta_1$  is shown in Fig. 15 (b).

#### IV. EXPERIMENTAL RESULTS

In this section, we show the experiments about the transition motion connected with vertical ladder climbing by MLR. The experimental condition is as follows:

- The ladder is set up vertically, and the interval of rungs on the ladder is constant 0.2 m with each other.
- The MLR upright stand in front of the ladder, and the distance from the robot to the ladder is 0.45 m.
- Cross section of rung is square of  $2 \times 2 \text{ cm}^2$  and is covered with a rubber plate for slip prevention.
- The intervals of rung on vertical ladder and horizontal ladder are respectively 20 cm and 40 cm.

The snapshots of transition motion from biped standing to ladder climbing are shown in Fig. 20. In this experiment, the robot can do the transition motion stably and smoothly. The error adjustment was included in the section of gripping the rung. The touch motion and gripping situation can be recognized through judging the vertical reaction forces of hands. The vertical forces are shown in Fig. 16(b), and the trajectory of COG will be adjusted according to the gripping situation (Fig. 16 (a)). In the transition motion from ladder

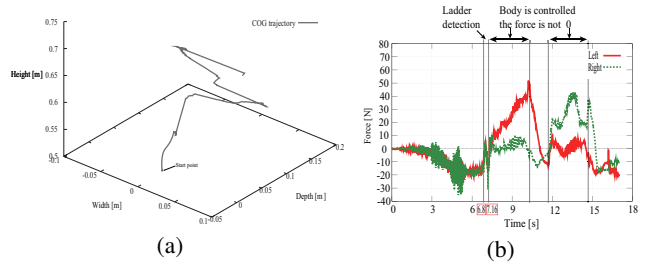


Fig. 16. Data of transition motion from biped standing to ladder climbing. (a) : Trajectory of robot's COG in walking close motion. (b): Contact force of two hands in the motion of walking close to ladder.

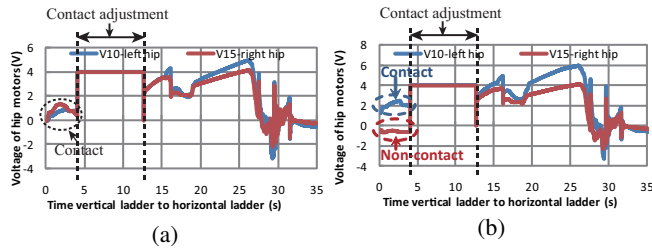


Fig. 17. Voltages of hip motors of transition motion from vertical ladder to horizontal ladder. (a) General initial situation. (b) Bad initial situation-right foot does come in contact with the ladder.

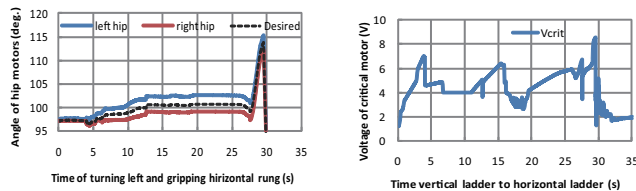


Fig. 18. Angle errors in turning shoulder motion.

Fig. 19. Max voltage of motors.

climbing to brachiation, the contact situation adjustment measure is also used for initial error adjustment. Fig. 17 (a) shows the hip motors' voltage in general situation. However, sometimes the robot cannot step on the ladder symmetrically. Fig. 17 (b) shows the right foot does not contact the rung. We call it as a bad initial situation. In this case, a big torque will load on left hip motor and that motor will be overloaded if there is no adjustment measure like Fig. 10 and Fig. 11. The experimental results with contact situation adjustment measure is shown in Fig. 17 (b)-bad initial situation. The non-symmetrical errors can be observed from the angle errors of hip joint (Fig. 18). According to the voltage of hip torques and the position errors in Fig. 18, we can find that the

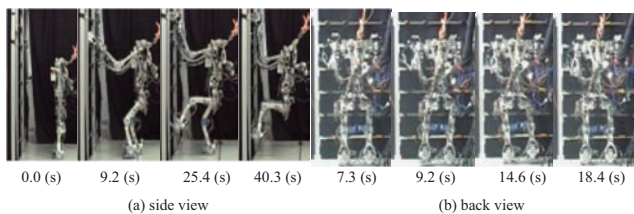


Fig. 20. Snapshots of motion video from biped standing to ladder climbing.

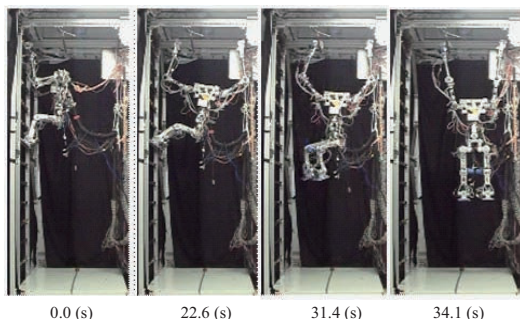


Fig. 21. Snapshots of transition motion from ladder climbing to brachiation.

left foot can supply the supporting force after the contact situation adjustment measure. The overload of right foot has been successfully prevented. The voltage of critical motor is shown in Fig. 19. That voltage is the maximum absolute value of all the motors. Since the voltage in Fig. 17 is in the safe range (0 V-10 V), we can conclude that all the motors are working in a safe condition. The snapshots of experimental video are shown in Fig. 20 and Fig. 21.

## V. CONCLUSIONS AND FUTURE WORKS

In this paper, two transition motions are designed for the multi-locomotion robot to carry out brachiation from a walking state. Error correction algorithms are proposed to cope with position errors at each transfer. Different reaction forces from expected force and excessive torque needed to perform the motion are used to detect the error situations. We confirmed that these transition motions with the error corrections successfully were robust and stable through some experiments with the multi-locomotion robot.

As a future work, the robot should be capable of sensing its environments such as interval of each rung on the ladder.

## REFERENCES

- [1] T. Takenaka, T. Matsumoto and T. Yoshiike, "Real time motion generation and control for biped robot," *Proc. of IEEE Int. Conf. on Robotics and Automation*, pp. 1594-1600, 2009.
- [2] S. Meek, J. Kim, and M. Anderson, "Stability of a trotting quadruped robot with passive, underactuated legs," *Proc. of IEEE Int. Conf. on Robotics and Automation*, pp. 347-351, 2008.
- [3] H. Nishimura and K. Funaki, "Motion control of three-link brachiation robot by using final-state control with error learning," *IEEE/ASME Trans. on Mechatronics*, Vol. 3, no. 2, pp. 120-128, 1998.
- [4] F. Kanehiro, H. Hirukawa, K. Kaneko, S. Kajita, K. Fujiwara, K. Harada, and K. Yokoi, "Locomotion Planning of Humanoid Robots to Pass Through Narrow Spaces" *Proc. of IEEE Int. Conf. on Robotics and Automation*, pp. 604-609, 2004.
- [5] T. Fukuda, T. Aoyama, Y. Hasegawa and K. Sekiyama, "Multilocomotion Robot: Novel Concept, Mechanism, and Control of Bio-inspired Robot" *Artificial Life Models in Hardware*, pp. 65-86, Springer, 2009.
- [6] T. Aoyama, Y. Hasegawa, K. Sekiyama and T. Fukuda, "Stabilizing and direction control of efficient 3-D biped walking based on PDAC," *IEEE/ASME Trans. on Mechatronics*, Vol. 14, no. 6, pp. 712-718, 2009.
- [7] T. Aoyama, K. Sekiyama, Y. Hasegawa, and T. Fukuda, "Optimal limb length ratio of quadruped robot minimizing joint torque on slope," *Applied Bionics and Biomechanics*, Vol. 6, no. 3-4, pp. 259-268, 2009.
- [8] H. Kajima, M. Doi, Y. Hasegawa and T. Fukuda, "A study on a brachiation controller for a multi-locomotion robot - realization of smooth, continuous brachiation," *Advanced Robotics* Vol. 18, no. 10, pp. 1025-1038, 2004.
- [9] H. Yoneda, K. Sekiyama, Y. Hasegawa and T. Fukuda, "Vertical ladder climbing motion with posture control for Multi-Locomotion Robot," *Proc. of IEEE/RSJ Int. Conf. on Intelligent Robots and System*, pp. 3579-3584, 2008.
- [10] K. Harada, S. Kajita, K. Kaneko, and H. Hirukawa, "ZMP analysis for arm/leg coordination," *Proc. of IEEE/RSJ Int. Conf. on Intelligent Robots and Systems*, Vol. 1, pp. 75- 81, 2003.
- [11] K. Harada, H. Hirukawa, F. Kanehiro, K. Fujiwara, K. Kaneko, S. Kajita and M. Nakamura, "Dynamic balance of a humanoid robot grasping an environment," *Proc. IEEE/RSJ Int. Conf. on Intelligent Robots and Systems*, pp. 1167-1173, 2004.
- [12] E. Yoshida, M. Poirier, J.-P. Laumond, O. Kanoun, F. Lamiraux, R. Alami and K. Yokoi, "Whole-body motion planning for pivoting based manipulation by humanoids," *Proc. of IEEE Int. Conf. on Robotics and Automation*, pp. 3181-3186, 2008.
- [13] K. Koyanagi, H. Hirukawa, S. Hattori, M. Morisawa, S. Nakaoka, K. Harada, and S. Kajita, "A pattern generator of humanoid robots walking on a rough terrain using a handrail," *Proc. of IEEE/RSJ Int. Conf. on Intelligent Robots and Systems*, pp. 2617-2622, 2008.